ACS Catalysis

Research Article

pubs.acs.org/acscatalysis

Catalysis and Reactivation of Ordered Mesoporous Carbon-Supported Gold Nanoparticles for the Base-Free Oxidation of Glucose to Gluconic Acid

Puyu Qi, Shasha Chen, Jin Chen, Jianwei Zheng, Xinlei Zheng, and Youzhu Yuan*

State Key Laboratory of Physical Chemistry of Solid Surfaces and National Engineering Laboratory for Green Chemical Production of Alcohols-Ethers-Esters, Collaborative Innovation Center of Chemistry for Energy Materials, College of Chemistry and Chemical Engineering, Xiamen University, Xiamen 361005, China

Supporting Information

ABSTRACT: An ordered mesoporous carbon (CMK-3)-supported gold catalyst was prepared and used in the aerobic oxidation of glucose to gluconic acid under base-free conditions with molecular oxygen. XRD and TEM results revealed that gold nanoparticles were uniformly dispersed on the surface and in the channels of CMK-3. Catalytic tests showed that conversion remarkably increased with decreased selectivity when oxygen pressure and reaction temperature were increased. Glucose conversion to gluconic acid reached over 92% with 85% selectivity under the conditions of 383 K reaction temperature, 0.3 MPa oxygen pressure, and 2 h reaction time. Hydrogen peroxide was generated during reaction, and the relationship between hydrogen peroxide and the byproduct fructose was discussed. Low glucose/Au molar ratio minimized fructose formation. A 92% gluconic acid yield was obtained after reaction for 15 min when the molar ratio of glucose/Au was set to 100. The spent catalyst treated with an aqueous solution of NaOH at 363 K could produce glucose conversion up to 87%, which was close to the result of as-prepared catalyst and excluded the effect of alkaline residues.

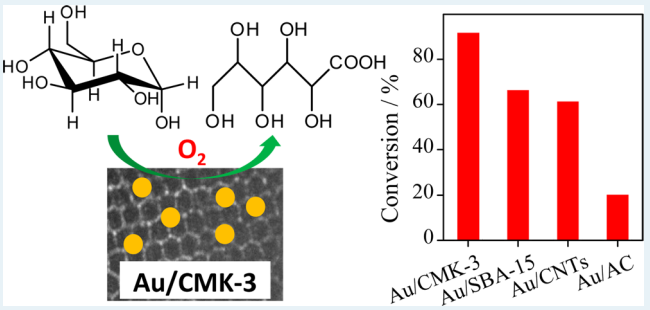

KEYWORDS: *gold, mesoporous carbon, glucose oxidation, base-free condition, gluconic acid*

1. INTRODUCTION

The transformation of biorenewable feedstock to highly attractive chemical intermediates is becoming an effective method of minimizing pollution and improving the efficiency of energy utilization.[1,2] Gluconic acid, mostly produced from the selective oxidation of glucose, is widely used in many fields, including construction industries, food additives, pharmaceutical raw materials, and paper industries.[3−5] Gluconic acid is basically manufactured through fermentation using *Aspergillus niger* and *Gluconobacter suboxydan*, but economic and environmental problems may be a serious weakness in the case of large-scale production.[3,6,7] By contrast, heterogeneous catalysis for such transformation is receiving considerable attention because it is eco-friendly.[8−10] Developing heterogeneous catalysts as replacement for enzymes is becoming increasingly important.

In early reports, platinum (Pt) and palladium (Pd) were commonly used in this reaction with lead or bismuth as the second metal. Although beneficial effects were achieved with high selectivity and a conversion above 99%, low durability was observed from the leaching of the second metal.[10,11] Gold (Au) is also widely used in the aerobic oxidation of carbohydrates with high catalytic activity and selectivity.[12,13] Rossi and co-workers[14] studied the performance of Au/C for glucose oxidation under various reaction conditions and compared it with traditional Pt, Pd, and Pt/Pd bimetallic catalysts. The results revealed that the Au catalyst was obviously superior to others because it exhibited low sensitivity to oxygen poisoning. Another advantage of the Au catalyst was that it showed activity in a wide range of pH values.

The oxidation of glucose to gluconic acid was mostly undertaken under alkaline conditions because the presence of a base could significantly improve the catalytic activity.[15−17] Rossi et al.[14] found that the solution conditions could affect the stability of the catalyst because the decline degree of conversion was found to be related to the pH value in the recycling experiments. A relatively high pH condition (pH = 9.5) was beneficial for the stability without any leaching of Au. By contrast, almost 16% of the Au was lost when the pH was fixed at 7.0. The loss of Au and the aggregation of Au nanoparticles (Au NPs) could lead to a drastic drop in conversion after four runs.

Aside from carbon-supported catalysts, metal oxide supports have also been intensively researched.[18−21] A 0.45% Au/TiO_2 catalyst was tested for stability under 313 K, pH 9.0, and 250

Received: December 26, 2014
Revised: March 7, 2015

DOI: 10.1021/cs502093b
ACS Catal. 2015, 5, 2659−2670

mmol/L glucose concentration. The value of the turnover frequency generally stayed constant for 17 runs when the reaction time was prolonged for the last batches. Au NPs showed almost no agglomeration after the recycling experiments.[18] A 0.3% Au/Al_2O_3 catalyst was used in a continuous-flow system of glucose oxidation, showing outstanding performance and stability in 110 days of operation.[19] Wang et al.[20] studied the stability of Au supported on metal oxides for the base-free oxidation of glucose. Reactions were carried out at 338 K and 2.3 bar for 6 h with a glucose/Au molar ratio of 140. Approximately 30% and 60% decreases in conversion were observed for Au/n-CeO_2 (for nanosized CeO_2) and Au/μ-CeO_2 (for microsized CeO_2), respectively. According to the report, the relatively more stable nature of the Au/n-CeO_2 catalyst was due to the low surface density of Au NPs and more anchoring sites that could stabilize the Au NPs against particle growth.

Another factor that caused deactivation was the absorbed carboxylic acids, which could be removed by calcination. However, the calcination step would lead to a severe loss of activity because the diameter of the Au NPs was obviously larger than that of the as-prepared catalyst. Miedziak et al.[21] prepared 0.5% Au−Pd/MgO and carried out the reaction under a mild condition of 333 K and atmospheric pressure for 24 h. The highlight was the use of air as oxidant instead of pure oxygen, and the catalyst achieved a conversion of 62% under a base-free condition. However, the catalyst presented a drastic decrease in activity, giving a conversion of less than 20% in the second use. The conversion could be improved by only ∼5% through a calcination treatment. The author ascribed the catalyst deactivation to product inhibition and support dissolution.

The stabilities of the above-mentioned catalysts in the base-free oxidation of glucose are not satisfactory, and a useful regeneration method has not been established. In fact, except for glucose oxidation, gold catalysts also suffered from deactivation caused by carboxylic compounds or intermediates in the oxidation of carbohydrates such as octanol[22] and benzyl alcohol,[23] etc. Adding sacrificial base could effectively solve this problem; however, the addition of base would generally produce the corresponding salt instead of pure acid and cause difficulties to the post-treatment of the reaction liquid and therefore being environmentally unfriendly. The problem of corrosion and waste base disposal was also presented in the oxidation of aliphatic alcohols;[24] hence, developing a gold catalyst that has excellent performance and favorable stability for the base-free oxidation of carbohydrates is highly desired.

Given the high surface area and uniform mesopore size of the ordered mesoporous carbon, this material has been intensively explored as a catalyst support.[25−27] Ma et al.[2] discovered the superior performance of Au supported on ordered mesoporous carbon in the aerobic oxidation of glucose. The superior activity was ascribed to the mesopore system that could not be blocked by metal, and the remaining space was enough for the diffusion of molecules in the reaction. Thus, the contact between Au and glucose and the mass transfer of gluconic acid were facilitated.

Previously, Rossi et al.[14] reported that high temperature and pressure could improve the performance of Au/C catalyst, but they did not discuss the effects in detail. To clarify this effect, CMK-3, a kind of ordered mesoporous carbon, was chosen in the present study as the catalyst support to load Au NPs without any calcination step for the base-free oxidation of glucose to gluconic acid under different temperatures and pressures. The appearance of fructose was obviously odd because it was commonly produced under alkaline conditions in this reaction. By eliminating the fructose production and minimizing it at the bottom, a gluconic acid yield of ∼92% could be achieved. Furthermore, the catalyst stability and different regeneration methods were studied intensively. The results showed that the spent catalyst treated with an aqueous NaOH solution at 363 K could give a glucose conversion of 87%, which was quite close to that of the as-prepared catalyst and excluded the effect of alkaline residues.

2. EXPERIMENTAL SECTION

2.1. Catalyst Preparation. The preparation of SBA-15 followed the procedure described by Zhao et al.[28] The synthesis of CMK-3 was carried out using sucrose as the carbon source and SBA-15 as the hard template according to known procedures.[29] Briefly, 1.0 g of SBA-15, 1.25 g of sucrose, 5 g of deionized water, and 0.14 g of concentrated sulfuric acid were mixed. The mixture was successively treated at 373 and 433 K for 6 h. When the white mixture turned dark brown, another 0.8 g of sucrose, 5.0 g of deionized water, and 0.07 g of concentrated sulfuric acid were added. Afterward, thermal treatment was performed again. The black solid substance was calcined at 1223 K for 5 h with 2 K min^{-1} heating rate under argon. The silicon skeleton was removed with 30% hydrofluoric acid. Finally, the resultant mesoporous carbon material was filtered, washed several times with ethanol, and dried overnight at 383 K.

A suitable amount of the stabilizing agent sodium gluconate was added into 125 mL of diluted $HAuCl_4$ aqueous solution and stirred at room temperature for 4 h. Freshly prepared $NaBH_4$ aqueous solution was rapidly injected into the mixture. When the solution turned bright orange, CMK-3 was added. The solution was further stirred vigorously at room temperature for 2 h, filtered, and then washed with distilled water several times until no trace of chloride was found by the $AgNO_3$ test. The sample was finally dried overnight at 383 K for the activity test without calcination. Given that the stabilizing agent itself was a sodium salt, it was assumed to have only a slight influence, even if traces remained on the catalyst surface.

The other carbon supports including carbon nanotubes (CNTs), activated carbon (AC), graphite, and graphene were calcined at 1223 K under argon to remove the surface oxidation groups and keep the carbon supports similar to the CMK-3 support. Prior to thermal treatment, the as-received CNTs and AC were first purified with concentrated nitric acid (68 wt %) at 353 K for 16 h under refluxing to remove the residues left in the synthesis step, such as nickel and iron cations. Afterward, the treated CNTs and AC were washed with distilled water several times until the filtrate became neutral and dried overnight at 383 K. The graphite and graphene support were directly calcined at 1223 K without the nitric acid treatment because their purities were acceptable. The metal-loading step was completely the same as above. As for the preparation of Au/SBA-15 catalyst, SBA-15 was first functionalized with 3-aminopropyltriethoxysilane (APTES) to modify the surface group. The solid formed, which was named SBA-15-NH_2, was then stirred with $HAuCl_4$ aqueous solution for 30 min. A freshly prepared $NaBH_4$ solution was rapidly injected into the mixture. After stirring for another 1 h, the solution was filtered, washed, and dried overnight. For comparison, ZrO_2 support was prepared using $Zr(NO_3)_4$ as ingredient according to the

DOI: 10.1021/cs502093b
ACS Catal. 2015, 5, 2659−2670

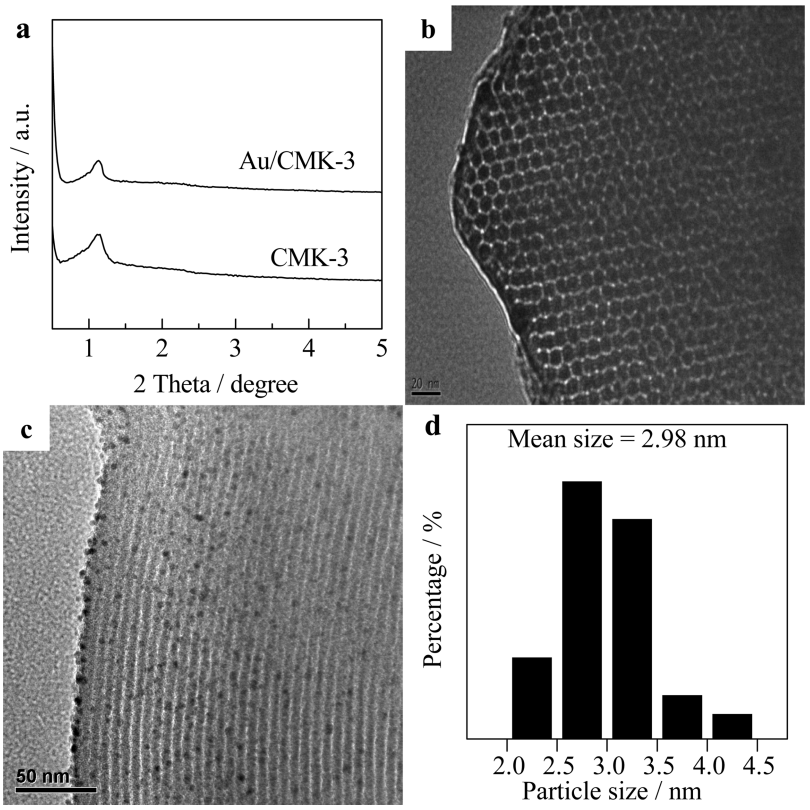

Figure 1. (a) Small-angle XRD patterns of CMK-3 and Au/CMK-3 catalyst; (b) TEM images of CMK-3; (c) TEM image of Au/CMK-3 catalyst; and (d) Au particle size distribution of Au/CMK-3.

procedure described in the literature.[30] A prepared ZrO_2 was mixed with $HAuCl_4$ aqueous solution, and then 0.1 mol L^{-1} ammonium hydroxide was added dropwise to adjust the pH to 9.0. After stirring for 2 h, the mixture was filtered and washed with a filter membrane and then dried overnight at 383 K. The pale yellow solid was finally reduced at 473 K for 2 h with 2 K min^{-1} heating rate under N_2/H_2 flow.

2.2. Catalyst Characterization. X-ray diffraction (XRD) patterns were obtained using a Rigaku Ultima IV equipped with Cu K_α radiation (λ = 0.15418 nm) scanned from 10° to 90°. The scanning rate was 10° min^{-1}, and the voltage and current were 35 kV and 15 mA, respectively.

N_2 adsorption−desorption isotherms were measured by the static volumetric method at 77 K using a Micromeritics TriStar II 3020 porosimetry analyzer. Prior to the measurements, all samples were degassed at 573 K for 4 h. The specific surface area (S_{BET}) was calculated according to the Brunauer−Emmett−Teller (BET) method, adopting the data within the relative pressure range P/P_0 of 0.05−0.2. The total pore volume was determined from the adsorbed amount of N_2 at a relative pressure of ∼0.995. The average pore diameter and pore size distributions were evaluated using the desorption branch of isotherm in line with the Barrett−Joyner−Halenda method.

Transmission electron microscopy (TEM) images were derived on a Philips Analytical FEI Tecnai 30 electron microscope operated at a 300 kV acceleration voltage. Before observation, the samples were ultrasonically dispersed for 30 min in ethanol at room temperature and then dropped on a carbon-coated copper grid. Ethanol was dried off under infrared light irradiation.

The exact Au loadings were calculated by inductively coupled plasma atomic emission spectrometry (ICP-AES) using an NCS Plasma1000. All the catalysts with carbon supports were calcined in a muffle furnace at 873 K (graphene and graphite at 1223 K, for they could not be burned away at 873 K) for 4 h with 2 K min^{-1} heating rate to remove the support. The remaining Au was dissolved with aqua regia at room temperature and further diluted with 5% HCl in a 25 mL volumetric flask before measurement. The Au/SBA-15 and Au/ZrO_2 catalysts were added into excess aqua regia and boiled for 20 min. The solution was syringed out and filtered after cooling down and similarly diluted with 5% HCl in a 25 mL volumetric flask.

The ultraviolet−visible (UV−vis) spectra were recorded on a Shimadzu UV2550 UV−vis spectrometer. The reaction mixture was syringe filtered with a microfiltration membrane (0.22 μm), and then 15 mL of the clarified solution was added into a volumetric flask and filled to 25 mL with excess titanyl sulfate. The solution turned yellow and was kept in a refrigerator prior to the measurement. A series of standard solutions (10, 20, 30, 40, and 50 μg mL^{-1}) were measured to quantify the exact amount of hydrogen peroxide.

Cyclic voltammetry (CV) experiments were carried out with a LabNet UI5020 electrochemical workstation with a three-electrode cell according to the method described in Cui's work.[31] A glassy carbon electrode was used as the working electrode. It was polished with alumina polishing powder (Gaoss Union, 0.05 μm) and ultrasonically treated with ultrapure water. This procedure was repeated three times before dropping the catalyst. A platinum electrode and saturated calomel electrode were used as the counter and reference electrodes, respectively. Exactly 10 mg of catalyst was added into the mixed liquor that contained 0.5 mL of ultrapure water, 0.45 mL of ethanol, and 0.05 mL of naphthol. The

DOI: 10.1021/cs502093b
ACS Catal. 2015, 5, 2659−2670

mixture was ultrasonically treated for 30 min and then coated onto the glassy carbon electrode. All experiments were conducted at room temperature under stirring. Current−time data were adopted when the current was stabilized.

Thermogravimetric analysis (TGA) was carried out on a TG_209F1 thermogravimetric analyzer. After drying overnight at 373 K, the catalysts were treated at 1073 K with 10 K min^{-1} heating rate in a nitrogen flow.

XPS measurements were conducted on a Phi Quantum 2000 Scanning ESCA Microprobe instrument using an Al Kα radiation source ($h\nu$ = 1486.6 eV). Prior to the measurements, each sample was pressed into a thin disk. The XPS spectra of all the samples were recorded at room temperature. The binding energy was calibrated using C 1s peak at 284.6 eV as reference with an uncertainty of ±0.2 eV.

The catalysts were also analyzed by CO_2 temperature-programmed desorption (CO_2-TPD) on a Micromeritics Autochem II 2920 instrument with a thermal conductive detector (TCD). All the tested catalysts were dried overnight at 383 K prior to the measurement. Typically, 40 mg of the catalyst sample was put into a quartz U tube, and CO_2 was passed through the catalyst bed for 1 h at room temperature. Weakly adsorbed CO_2 was removed by pure Ar sweeping until the baseline of TCD signal stabilized. Under an atmosphere of pure Ar with a rate of 50 mL min^{-1}, CO_2-TPD was conducted from room temperature to 973 K at a heating rate of 10 K min^{-1}.

2.3. Catalytic Testing. The catalytic performances were tested in a 48 mL pressure bottle. In a typical run, 20 mL of 0.1 mol L^{-1} aqueous glucose solution and 0.0396 g of catalyst were used. The system was first vacuumized with a vacuum pump and then fed with oxygen. This process was repeated several times before the reaction. In addition to the normal reaction time, the reaction was allowed to proceed for an additional 10 min to ensure that the system reached the exact reaction temperature. The bottle was rapidly immersed in a water bath to cool, and the oxygen was turned off at the same time to stop the reaction. Afterward, the reaction liquid was immediately syringed out, filtered, and analyzed using high-performance liquid chromatography (HPLC) (Shimadzu LC20A) with glycol as internal standard. The HPLC was equipped with a Shodex Sugar Column (SH 1011) and a refractive index detector.

In all cases, the catalysts were recovered after reaction by centrifuging for 5 min (3000 rpm). The black solid was washed with distilled water several times until the supernatant became neutral. The washed catalysts were dried at 383 K for at least 4 h prior to reuse.

3. RESULTS AND DISCUSSION

3.1. Catalyst Characterization. The physical properties and morphology of the mesoporous carbon CMK-3 were studied by a series of characterizations. An ordered 2D-hexagonal structure was represented in the small angle XRD patterns in Figure 1, which was well maintained even after Au loading. Typical *P6mm* symmetry structure could also be observed in the TEM images. In addition, Au NPs that were uniformly dispersed on the surface and in the mesopore channels of the CMK-3 support could clearly be identified. The N_2 adsorption−desorption isotherms and pore size distribution patterns are shown in Figure S1. The obvious hysteresis loops also verified the typical mesostructure of the material. The support showed a BET surface area of ∼1110 m^2 g^{-1}, and the value decreased to 956 m^2 g^{-1} after loading about 1% Au (Table 1 and Table S1). This result confirmed that a part of the Au was confined in the pore channels. The XRD patterns in Figure S2 show that Au NPs were uniformly dispersed on other supports, such as SBA-15, ZrO_2, CNTs, graphite, and graphene, because no obvious peak belonging to Au species could be seen.

Table 1. Structural Properties of the Tested Catalysts

sample	S_{BET}, m^2 g^{-1}	V_{total}, mL g^{-1}	V_{meso}, mL g^{-1}	D_{meso}, nm	Au content, %	D_{Au}, nm
Au/CMK-3	956	1.17	0.84	4.0	0.94	2.98
Au/SBA-15	491	0.62	0.51	4.6	0.91	3.56
Au/CNTs	128	0.38	0.34	12.5	0.96	2.92
Au/graphene	34.2	0.12	0.11	9.2	0.83	3.22
Au/graphite	11.6	0.04	0.03	10.3	0.86	3.73
Au/AC	778	0.44	0.16	4.0	0.89	3.50
Au/ZrO_2	29.0	0.01	0.005	42.6	0.95	2.52

Furthermore, a strong glucose response was observed for the Au/CMK-3 catalyst by CV. Figure 2 shows the CVs data of 0.1 mol L^{-1} NaOH with 18 mmol L^{-1} glucose for different carbon catalysts. A strong cathodic peak at about −0.6 V could be observed for the Au/CNTs catalyst, regardless of the existence of glucose. To check the origin of this peak, we tested the cyclic voltammogram of pure CMK-3 and CNTs in NaOH without glucose, and the results are presented in Figure S3a. Obviously, both of them exhibited almost the same CV shape as the corresponding catalysts, indicating the cathodic peak at about −0.6 V originated from the CNTs. The peak at −0.6 V was considered because the electrochemical reduction of oxygen existed in the NaOH solution.[32] Because all the carbon supports were calcined at 1223 K under argon, their surface chemical properties were supposed to show little difference. Previously, it was reported that the CNTs exhibited more excellent catalytic activity than graphite in the electrochemical reduction of oxygen in KOH solution because of the cracks existing on the surface of the CNTs.[32] The roughness (for example cavities and cracks) of the electrode surface was also reported to affect the interactions with analytes in solution.[33] For the four different carbon supports, CNTs were meant to be advantageous in the electrochemical reduction of oxygen because of the fishbone-shaped structure in Figure S3b which was supposed to bring in more defects on the surface. In addition, we could see that except for the Au/CNTs catalyst, the Au/graphite catalyst also exhibited a small peak at about

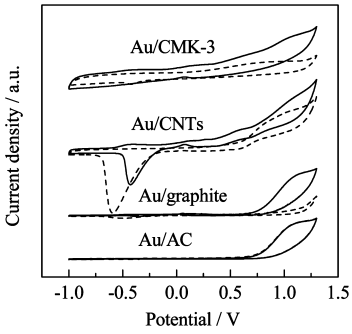

Figure 2. Cyclic voltammetric responses to 0.1 mol L^{-1} NaOH with 18 mmol L^{-1} glucose (solid line) and to 0.1 mol L^{-1} NaOH without glucose (dotted line) for different catalysts.

DOI: 10.1021/cs502093b
ACS Catal. 2015, 5, 2659−2670

−0.5 V. Considering the morphology of graphite, this might be ascribed to its layer structure, which would cause defects on the edge of each layer. By contrast, the border of CMK-3 and AC were relatively more saponaceous, thus being disadvantageous in the electrochemical reduction of oxygen. The glucose oxidation peak currents for the Au/CMK-3 and Au/CNTs catalysts were much larger than those of the Au/graphite and Au/AC catalysts. The anodic sweep began at −0.6 V for the Au/CMK-3 catalyst, which was more negative than that of the others. Therefore, the Au/CMK-3 and Au/CNTs catalysts have potential for the selective oxidation of glucose.

3.2. Catalytic Results. Table 2 summarizes the catalytic performances of several catalysts, including Au supported on

Table 2. Base-Free Oxidation of Glucose with Au NPs Supported on Different Carriers[a]

		selectivity, %			
catalyst	conv, %	gluconic acid	fructose	others	TOF[b] s^{-1}
Au/CMK-3	92.4	87.5	7.4	5.1	4.92
Au/SBA-15	67.0	92.4	3.8	3.8	4.76
Au/CNTs	62.0	82.7	15.5	1.8	2.40
Au/graphene	55.6	74.0	11.0	15.0	1.75
Au/graphite	54.5	84.1	10.6	5.3	1.68
Au/AC	20.8	91.4	6.1	2.5	0.61
Au/ZrO_2	12.7	91.9	5.6	2.5	0.35

[a]Reaction conditions: glucose = 0.36 g, H_2O = 20 mL, catalyst = 0.0396 g, glucose/Au (molar ratio) = 1000/1, T = 383 K, $P(O_2)$ = 0.3 MPa, reaction time = 2 h. [b]Calculated by the conversion at 5 min.

CMK-3, SBA-15, ZrO_2, CNTs, graphite, and graphene for the base-free oxidation of glucose. Because the exact Au amount was less than the theoretical one, the TOF values of these catalysts were calculated. On the basis of the data in Table 2, the catalytic activity of Au/CMK-3 was much better than those of the other chosen materials. A correlation could be observed that the conversion of glucose was basically positively correlated to the volume of mesopore (Table 1). This phenomenon might have resulted because the mesostructure could facilitate the contact between glucose molecules and Au NPs. In addition, the mass transfer process was also favored. The mesopore size of Au/CMK-3 was ∼4.0 nm, which was slightly larger than the average size of Au NPs. According to the theoretical model,[2] mesopores with a suitable size that are partially occupied by Au NPs but still have space for the diffusion of glucose and gluconic acid molecules would show a good activity. Among all the tested catalysts, only Au/CMK-3 and Au/AC had the most suitable pore size of 4.0 nm. Given that the mesopore volume of AC was too low, CMK-3 was obviously the most beneficial support for the reaction. The Au/SBA-15 catalyst, which had a pore size of 4.6 nm, also showed a satisfactory conversion of ∼70%. Particularly, the TOF value with the Au/SBA-15 catalyst was 4.76 s^{-1}, which meant that the reaction proceeded quite fast in the initial stage; however, the final conversion over it was 20% lower than the Au/CMK-3 catalyst, indicating the glucose oxidation was retarded for the rest of the reaction time. The reason will be discussed in Section 3.3.

A series of experiments were carried out over a range of different temperatures and pressures using Au/CMK-3 as catalyst. On the basis of the data in Table 3, increasing the temperature could effectively improve glucose conversion. No byproduct was produced when the reaction temperature was

Table 3. Catalytic Behaviors of Au/CMK-3 Catalyst for Base-Free Oxidation of Glucose under Different Temperatures and Oxygen Pressures[a]

		selectivity, %		
temp, pressure	conv, %	gluconic acid	fructose	others
333 K, 0.1 MPa	22.5	100	0	0
333 K, 0.3 MPa	29.3	100	0	0
363 K, 0.1 MPa	59.2	93.7	4.5	1.8
363 K, 0.3 MPa	73.1	92.1	5.1	2.8
383 K, 0.1 MPa	66.3	90.1	6.4	3.5
383 K, 0.3 MPa	92.4	87.5	7.4	5.1

[a]Reaction conditions: glucose = 0.36 g, H_2O = 20 mL, catalyst = 0.0396 g, glucose/Au (molar ratio) = 1000/1, reaction time = 2 h.

relatively low, which was consistent with the results in references;[14,34] however, as the temperature increased, certain byproducts appeared. Among them, fructose was the most dominant. According to previous reports,[14,34] fructose was produced through the isomerization of glucose, which occurred only under alkaline conditions. Given that no sacrificial base was added into the reaction system, the appearance of fructose was worth discussing. The same tendency was also observed with regard to pressure. The improvement was more obvious when the reaction pressure was increased at a high temperature. When the temperature was relatively low at 333 K and the pressure was increased from atmospheric pressure to 0.3 MPa, the conversion ascended from 22% to 29%. However, the enhancements were 14% for 363 K and 26% for 383 K, indicating that high conversion is achieved much more easily with the combination of high temperature and pressure compared with increasing only one of them. However, with gradually increasing pressure, the selectivity toward gluconic acid showed a measurable reduction. The reason why fructose was generated and its relationship with the reaction conditions would be discussed hereinafter.

3.3. Catalyst Deactivation and Regeneration. Recycling experiments were conducted to investigate the stability and deactivation of the catalyst. Figure S4 shows the conversion and selectivity data of four subsequent runs under the reaction conditions of 383 K and 0.3 MPa. Compared with the performance of catalysts in previous works[20,21] under base-free conditions, the Au/CMK-3 catalyst was relatively more favorable; however, its activity eventually decreased to a certain degree and had a conversion of 70% at the fourth run.

Because of the large specific surface area and the poor hydrophilicity of CMK-3 support, the mass loss of the catalyst was actually very serious through the washing steps, which was considered as one of the main reasons why the conversion of glucose dropped from 92% in the first run to 70% in the fourth run. In general, ∼30% mass loss of the catalyst was observed after the consecutive four runs, so the actual weight of catalyst in the fourth run could be regarded as about 0.03 g $\{0.0396 \times (1-0.3) \approx 0.03\}$. We carried out a comparison experiment with 0.03 g of fresh catalyst to evaluate the impact of weight loss and achieved a conversion of 87%, which was a little lower than 92% but much higher than 70%. Hence, we could say that the mass loss of the catalyst was actually a factor that caused the decrease of conversion, although not the crucial one.

To explore the other factors that cause deactivation, TEM and ICP-AES measurements were carried out to test the size and content of Au. The results of the particle size distribution in Figure 3 (more than 100 particles were accounted) revealed

DOI: 10.1021/cs502093b
ACS Catal. 2015, 5, 2659−2670

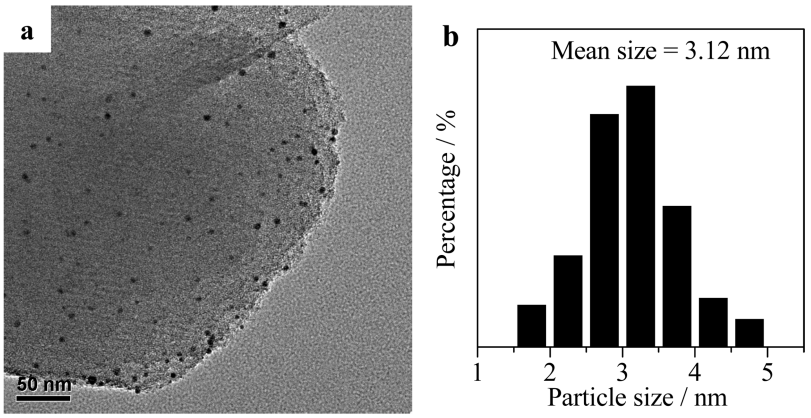

Figure 3. (a) TEM image of Au/CMK-3 catalyst after reuse for four runs; (b) Au particle size distribution of Au/CMK-3 catalyst after reuse for four runs.

that Au NPs grew in a very small degree after the reaction. The difference at this level could just be ignored, considering the system and human errors. The ICP-AES results indicated that 30% of Au was lost after four runs. However, given that the adsorption of carboxylic compounds was commonly observed in the selective oxidation of alcohols to acids, gluconic acid might occupy a certain weight in the tested sample. Hence, this result was not that accurate.

To eliminate the negative influence of the adsorbed carboxylic acids, two possible methods were assumed, and their regenerating effects were compared. The used catalysts were divided into two groups. One group was treated with NaOH aqueous solution. Exactly 0.12 g of used catalyst was added into 50 mL of 0.1 mol L^{-1} NaOH, and the mixture was stirred for 30 min at room temperature, 323, and 363 K, separately. These catalysts were centrifuged later and washed with distilled water until the supernatant became neutral. Finally, they were dried overnight at 383 K. The other group was calcined at 773 K for 5 h with 4 K min^{-1} heating rate under argon and nitrogen, separately.

The TGA curves in Figure 4 show the thermal weight loss of fresh, used, and all the recovered catalysts. It has reported[35,36] that the weight loss from room temperature to 423 K corresponds to the evaporation of residual water, the fell stage at 423 to 623 K belongs to the decarboxylation of carboxylic groups, the third stage between 623 and 773 K corresponds to the elimination of hydroxyl functionalities, and the last thermal decline is caused by the degradation of disordered or amorphous carbon. The weight loss percentages at different stages are respectively arranged in Table 4 according to the above information.

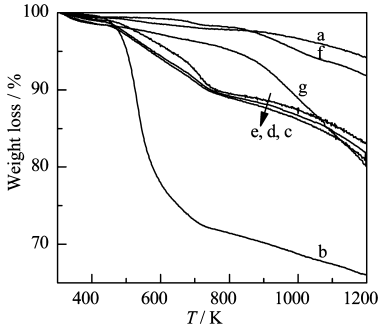

Figure 4. TGA curves of (a) fresh Au/CMK-3 catalyst; (b) the Au/CMK-3 catalyst after reuse for four times; (c) sample b treated with NaOH aqueous solution at 298 K; (d) sample b treated with NaOH aqueous solution at 323 K; (e) sample b treated with NaOH aqueous solution at 363 K; (f) sample b calcined at 773 K in argon; and (g) sample b calcined at 773 K in nitrogen atmosphere.

Table 4. Weight Loss of Fresh, Used, and Recovered Au/CMK-3 Catalysts at Different Temperature Ranges[a]

		weight loss at different temperature ranges, wt %			
treatment condition		RT−423 K	423−623 K	623−773 K	>773 K
fresh		0.7	0.9	0.6	1.9
used		0.5	23.1	4.7	4.0
NaOH treatment	RT	1.6	5.1	4.0	4.6
	323 K	1.1	5.2	4.2	4.1
	363 K	1.6	4.4	3.8	4.0
calcination treatment	773 K in Ar	0.6	0.5	0.8	4.5
	773 K in N_2	1.6	1.5	1.3	9.7

[a]Assignments for the species at different temperature ranges: RT−423 K, residual water; 423−623 K, carboxylic groups; 623−773 K, hydroxyl groups; >773 K, amorphous carbon.

A comparison between the fresh and used catalysts clearly shows that the amount of both surface carboxylic and hydroxyl groups increased. Particularly, the carboxylic groups gained their amount quite largely from only 0.9% to 23.1%. This result was direct and obvious proof that the produced carboxylic compounds were strongly adsorbed on the surface of the catalyst. It might remind us of the previous problem that, with a higher initial TOF value of 4.72 s^{-1}, the Au/SBA-15 catalyst yet exhibited a relatively lower conversion than Au/CMK-3 at final. Because the adsorption of carboxylic acid was severe in this reaction, considering the APTES modifying procedure through catalyst preparation, the abundant surface amino groups might help adsorb more acidic compounds and accelerate catalyst deactivation. Actually, we have also prepared the Au/SiO_2 catalyst with the same modifying step using APTES and tested the catalytic activity under identical reaction conditions. Because of its large mesopore volume (1.03 mL g^{-1}), the conversion was supposed to be considerable. However, the same phenomenon as with the Au/SBA-15 catalyst could be observed, although the conversion was 37.9% at a time of 5 min, and it increased only to 74.9% at 2 h. Furthermore, the

DOI: 10.1021/cs502093b
ACS Catal. 2015, 5, 2659−2670

quantity of disordered carbon doubled from 1.9% to 4.0%, which was possibly caused by the physical damage of vigorous stirring during the subsequent runs, and it was not affected by either NaOH or calcination treatment. Concerning the removal of carboxylic groups, the effects were all favorable. For the NaOH treatment group, the residue of the carboxylic group was almost the same in number for the catalysts treated at room temperature and 323 K. However, the value for the 363 K sample was lower, possibly because the carboxylic compounds were strongly adsorbed, and a high temperature was necessary to break the force acting between the compounds and catalyst surface. Although a gap still existed between the recovered catalyst and the fresh catalyst, the used catalyst showed significant improvement. The hydroxyl group formed through the reaction was almost not influenced by the NaOH treatment, as expected. By contrast, the calcination group showed good performance in removing both carboxylic and hydroxyl groups, especially for the catalyst calcined under argon, which had almost the same weight loss as the fresh catalyst.

From the TEM images and size distributions of Au NPs in Figure S5, the sizes of Au NPs in the NaOH treatment group remained almost constant as the used catalyst at ∼3.0 nm. However, the calcination group showed larger sizes of over 3.5 nm. The value might not seem to increase very noticably, but some extraordinary large particles that appear in these two catalysts indicated that agglomeration truly happened. The 20 nm scale TEM images in Figure S5g,h clearly show that these particles could achieve a size of over 15 nm, which could not be found in other catalysts. Furthermore, the ICP-AES results showed that the recovered catalysts had a much higher Au content than the used one, thereby confirming our previous assumption that the relatively low amount of Au for the used catalyst was caused mainly by the occupation of the adsorbed carboxylic compounds.

The conditions of the surface elements analyzed with XPS are discussed below. The XPS spectra of Au 4f are shown in Figure 5a and fitted into two peaks. A study has reported[37] that the binding energies of Au $4f_{5/2}$ and Au $4f_{7/2}$ were located at 87.7 and 83.9 eV for Au^0 and at 89.6 and 86.3 eV for Au_2O_3, respectively. For the fresh catalyst, the peaks were located at 84.5 and 88.2 eV, revealing the valence of Au species between 0 and +3. After the experiments, the peaks shifted slightly to the high binding energy right at 84.7 and 88.4 eV, which might possibly be explained by the abundant oxygen atoms with stronger electron negativity than the carbon existing in the adsorbed carboxylic acids. However, the peaks returned to 84.5 and 88.2 eV after regeneration (the catalyst treated by NaOH at 363 K was chosen here).

The O 1s spectra in Figure 5b could be divided into four peaks as reported.[38] The carbonyl oxygen of quinones was located at 531−531.9 eV; the carbonyl oxygen atoms in esters and anhydrides and the oxygen atoms in phenolic groups at 532.3−532.8 eV; the noncarbonyl oxygen atoms in esters and anhydrides at 533.1−533.8 eV; and the COOH at a binding energy of 534.3−535.4 eV. The peak area of the used catalyst was relatively much bigger than that of the fresh one, indicating that a large amount of oxygen atoms exists in the catalyst. However, it was significantly reduced after the NaOH treatment but was still slightly larger than that of the as-prepared catalyst. The peak that corresponds to COOH at 534.1 eV was quite small and took only ∼5% in the fresh catalyst. After the reactions, it rose to 21%, obviously because of the strongly adsorbed carboxylic acids. Meanwhile, the peak

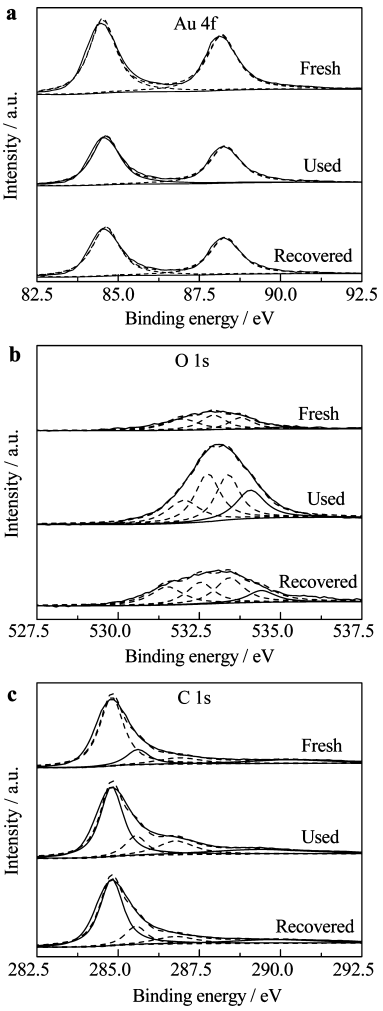

Figure 5. XPS spectra of (a) Au 4f, (b) O 1s, and (c) C 1s of the catalysts of fresh, reused four times, and regenerated with NaOH aqueous solution at 363 K.

area that corresponds to the carbonyl oxygen in quinones dropped drastically from 35% to 20%.

According to Wan et al.,[39] different surface groups affect the reaction to a great extent. For example, the carbonyl of quinones and phenol groups could promote the adsorption of reactants and intermediates, thereby becoming beneficial for the reaction. However, the carboxyl groups had an opposite effect and were unfavorable for the product formation. After the NaOH treatment at 363 K, the peak area percentage of COOH dropped to 14%, which means that about half of the adsorbed carboxylic compounds were removed. Meanwhile, the peak of the carbonyl oxygen of quinones returned to ∼27%.

In Figure 5c, the C 1s spectra could also be resolved into four peaks.[40] The sp^2-hybridized graphitic carbon was located at 284.5 eV; the carbon atoms in the C−O single bond of phenols and ethers, at 286.1 eV; the carbon atoms doubly bonded to the oxygen in ketones and quinones, at 287.5 eV; and the carbon in the C═O of carboxyls, carboxylic anhydrides, and esters, at 288.7 eV. The graphitic carbon formed the majority of ∼65% in the fresh catalyst, whereas the latter two peaks comprised 23% of the area. As expected, the proportion of the carbonyl in ketones, quinones, and carboxylic compounds increased in quantity to ∼32% after the recycling experiments, and as a result, the area percentage of the sp^2-hybridized graphitic

DOI: 10.1021/cs502093b
ACS Catal. 2015, 5, 2659−2670

carbon dropped to 54%. As surmised, the NaOH treatment would be quite useful to remove the adsorbed carboxylic acids, as clearly seen in the spectra. The newly brought in C═O species through the reactions was clearly eliminated and took the share back to 25%, which was close to that of the fresh catalyst. At the same time, the area percentage of graphitic carbon returned to 60%. The proportion of the carbon singly bonded to oxygen was almost constant in the range of 13−15% throughout the entire process.

All recovered catalysts were tested with the same weight and reaction conditions as the fresh catalyst. Their regenerating performances listed in Figure 6 show that the NaOH treatment

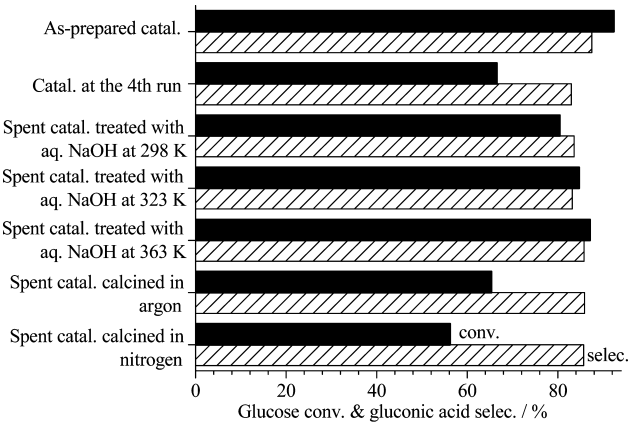

Figure 6. Conversion of glucose and selectivity of gluconic acid over catalysts as-prepared, reused four times, and regenerated using different methods. Reaction conditions: glucose = 0.36 g, H_2O = 20 mL, catalyst = 0.0396 g, glucose/Au (molar ratio) = 1000/1, T = 383 K, $P(O_2)$ = 0.3 MPa, reaction time = 2 h.

made significant improvements in the activity. The samples treated at 363 K showed the best conversion of over 87%, which was close to that of the fresh catalyst, and the result was consistent with the above characterizations. Given that the increase in activity might be affected by the promotion of surface basicity, the fresh catalyst was treated in the same way with NaOH at 363 K. After treatment, the catalyst showed a slightly reduced conversion, which was within the margin of error. Hence, the result revealed that the excellent activity of the recovered catalyst was not caused by the added basic sites. This conclusion was also confirmed by the CO_2-TPD experiment (Figure S6). The as-prepared Au/CMK-3 catalyst showed an almost negligible TCD signal at ~713 K whenever a prior CO_2 purge was given. The weak peak at ~713 K is essentially due to the decomposition of oxygen-containing species such as carboxyl and carbonyl groups rather than the contribution of CO_2-adsorption species on the catalyst surfaces. The spent catalyst after the NaOH treatment also represented a similar peak with negligible TCD intensity, indicating that no enhancement in the surface basicity occurred in this case. In contrast to the superior effects of the NaOH treatment, the calcination did not show any improvement on activity either under argon or nitrogen atmosphere, which might be ascribed to the agglomeration of Au NPs.

3.4. Mechanism Aspect. The above research demonstrated that the Au/CMK-3 catalyst had an advantage in the base-free oxidation of glucose and was very convenient to regenerate with NaOH treatment. Hence, the details of the reaction mechanism were studied to address questions concerning why fructose could be produced under acidic conditions. To illuminate the reaction path to the byproduct fructose, the amount of hydrogen peroxide produced in the reaction system was quantitatively measured. Given that hydrogen peroxide can react with titanyl sulfate and form a yellow complex, which has a strong adsorption at approximately 410 nm in UV−vis (Figure 7), the peak intensity can be

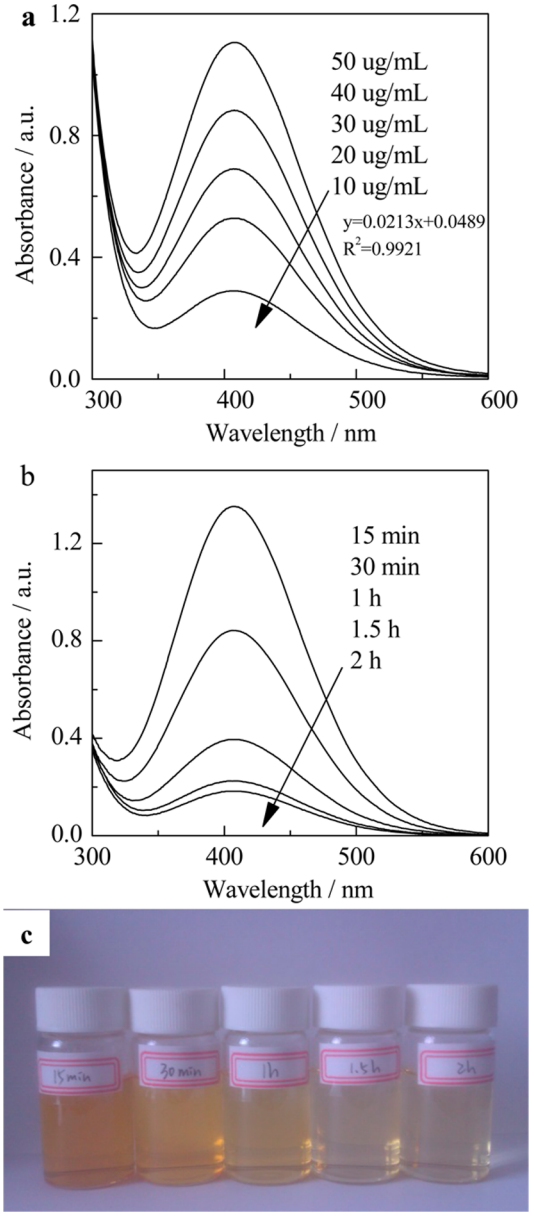

Figure 7. UV−vis spectra of the mixture of titanyl sulfate with (a) standard solutions and (b) reaction liquid at different reaction times; (c) the photograph of the mixture of titanyl sulfate with reaction liquid at different reaction times.

converted into concentration using the standard curves and fitted equation. According to the data in Table 5, as the reaction time lapsed with the gradually increasing conversion, the selectivity toward gluconic acid tapered off regularly. At the same time, the concentration of hydrogen peroxide also dropped drastically, in keeping with the variation tendency of the gluconic acid selectivity. This phenomenon could also be observed intuitively in Figure 7c, which presents the photo-

DOI: 10.1021/cs502093b
ACS Catal. 2015, 5, 2659−2670

Table 5. Base-Free Oxidation of Glucose and Concentration of Hydrogen Peroxide Found over Au/CMK-3 Catalyst As a Function of Reaction Time[a]

		selectivity, %			
reaction time, min	conv, %	gluconic acid	fructose	others	concn $(H_2O_2)_{found}$, mmol L^{-1}
15	53.0	94.6	4.1	1.3	1.80
30	63.8	94.0	4.8	1.2	1.10
60	79.6	91.2	5.5	3.3	0.48
90	88.4	89.5	6.7	3.8	0.24
120	92.4	87.5	7.4	5.1	0.18

[a]Reaction conditions: glucose = 0.36 g, H_2O = 20 mL, catalyst = 0.0396 g, glucose/Au (molar ratio) = 1000/1, T = 383 K, $P(O_2)$ = 0.3 MPa.

graph of the mixture of the reaction liquid and titanyl sulfate. When the conversion reached ~93% in 2 h, which meant the completion of the reaction, the amount of hydrogen peroxide left was 0.18 mmol L^{-1}, and the mixture also turned almost colorless.

According to a previous report,[16] when glucose molecules react with oxygen and water, aside from gluconic acid, hydrogen peroxide is also produced. Thus, the more rapidly the main reaction occurs, the more hydrogen peroxide is produced. The author proved that the generated hydrogen peroxide would act as an oxidant to oxidize glucose and decompose to oxygen. However, apart from these two consumption reactions, hydrogen peroxide could also produce hydroxyl ions on the surface of Au by a series of chain reactions.[41] The isomerization reaction between glucose and fructose occurs only under the effect of hydroxyl ions. Given that no alkaline was added into the system in advance, and the reaction liquid became acidic because of the generated gluconic acid, the needed hydroxyl ions for the production of fructose could be afforded by hydrogen peroxide. This deduction was also confirmed by the results of the comparison experiments carried out at 383 K and 0.3 MPa. When no catalyst was added, no gluconic acid was produced. Consequently, no hydrogen peroxide was formed, and no fructose would be generated. Indeed, fructose formation was not observed in the actual situation. However, when extra alkaline was added into the system in the absence of catalyst, fructose was generated as the major product without any oxidizing products. This phenomenon indicated that fructose was produced with existing hydroxyl ions, and if no sacrificial alkaline was added into the system, fructose formation depended on the generated hydroxyl ions from hydrogen peroxide. The proposed model for reaction mechanism is presented in Figure 8.

From the variation tendency of hydrogen peroxide concentration and gluconic acid selectivity in Table 5, a corollary that in the inception phase, the main reaction had a comparatively fast rate and a great advantage over the isomerization reaction might possibly be obtained. Thus, the gluconic acid selectivity and the hydrogen peroxide concentration were relatively high at the reaction time of 15 min. However, as the reaction proceeded, given the decrease in reactant concentration and the deactivation of the catalyst, the main reaction was retarded, which could be observed from the pH course in Figure S7, and the accumulated hydrogen peroxide offered a favorable environment for glucose isomerization. As a result, the disparity between oxidation and isomerization became small. Accordingly, both the selectivity toward gluconic acid and the amount of hydrogen peroxide became less simultaneously. From a certain perspective, isomerization relied on oxidation, and the amount of fructose was positively correlated with the reaction conversion. This conclusion could be set up only when the catalyst was fixed. Because various catalysts would have different performances for the glucose oxidation reaction, we could predict that for two catalysts that achieved the same final conversion, the one that consumed less time would have better selectivity. For example, if the performances of the Au/CMK-3 and Au/CNTs catalysts were compared, the conversions were clearly almost the same

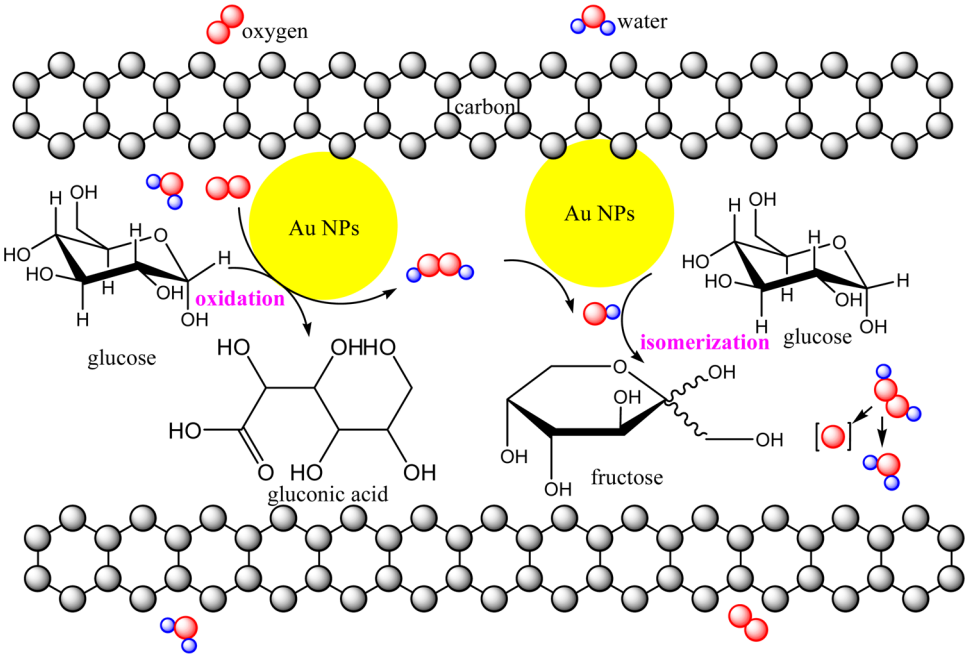

Figure 8. Proposed reaction mechanism for the base-free oxidation of glucose with molecular oxygen.

DOI: 10.1021/cs502093b
ACS Catal. 2015, 5, 2659−2670

for Au/CMK-3 at 30 min and for Au/CNTs at 2 h, whereas the gluconic acid selectivities showed a disparity of over 10%.

To prove the earlier point of hydrogen peroxide generation and consumption, a series of experiments were carried out. Solutions of 0.05 mol L^{-1} H_2SO_4 and 0.1 mol L^{-1} NaOH were used to adjust the initial pH of the reaction liquid, and the connection of conversion, selectivity, and the amount of hydrogen peroxide were studied. The data in Table 6 indicate a

Table 6. Oxidation of Glucose over Au/CMK-3 Catalyst at Different Initial pH Conditions[a]

condition	H^+ (or OH^-)/glucose, molar ratio	conv, %	selectivity (gluconic acid), %	concn $(H_2O_2)_{found}$, mmol L^{-1}
H_2SO_4	1	16.1	98.2	0.95
	0.5	19.2	98.0	1.19
	0.1	41.8	97.1	1.41
	0	53.0	94.6	1.80
NaOH	0.1	70.7	89.3	1.26
	0.5	90.7	66.1	0.63
	1	92.6	63.6	0.14

[a]Reaction conditions: glucose = 0.36 g, H_2O = 20 mL, catalyst = 0.0396 g, glucose/Au (molar ratio) = 1000/1, T = 383 K, $P(O_2)$ = 0.3 MPa, reaction time = 15 min.

volcano-type change in the amount of hydrogen peroxide with the increase in initial pH. As the amount of H_2SO_4 gradually increased, as expected, glucose conversion dropped drastically because the main reaction was intensively suppressed. As mentioned previously, hydrogen peroxide was produced in the oxidation reaction; consequently, the concentration of hydrogen peroxide was relatively low, and isomerization suffered, as well, leading to the tremendous gluconic acid selectivity. When alkaline was added, oxidation was promoted, as Rossi et al.[14] reported, and glucose conversion increased to a large extent. Similarly, the selectivity decreased as a result. At an initial pH of 13.0, the reaction was fast, such that almost full conversion was achieved at the reaction time of 15 min, with ~60% selectivity; however, despite the facilitated main reaction, the detected hydrogen peroxide was extremely low because the generated hydrogen peroxide was largely decomposed to oxygen under the effect of added hydroxyl ions, as Rossi et al. proved.[16]

With regard to the influence of temperature and pressure, both of them could affect the selectivity to gluconic acid when the main reaction was facilitated. A comparison of the data of the reactions at 363 K and 0.1 MPa for 2 h and at 383 K and 0.3 MPa for 30 min show that although the conversion of the latter was higher, the selectivity was also better. Similar to the law that catalysts with better activity also have better selectivity, a reaction condition beneficial for conversion would also have benefits for selectivity. From this aspect, obtaining both high conversion and selectivity is desirable, and the feasible way is to finish the reaction as soon as possible. This process can be optimized by increasing the temperature or pressure, shortening the reaction time, and reducing the glucose/catalyst molar ratio simultaneously. To verify this deduction, a series of experiments with different glucose/Au molar ratios were conducted, and the results are listed in Table 7, which shows an obvious consistency with the above inference. When the glucose/Au ratio was decreased to 500, the reaction consumed ~1 h to achieve 99% conversion with 88% selectivity. More remarkably, almost full conversion and approximately 92% selectivity were obtained in only 15 min when the ratio was set to 100.

Table 7. Base-Free Oxidation of Glucose over Au/CMK-3 Catalyst under Different Glucose/Au Molar Ratios[a]

glucose/Au, molar ratio	reaction time	conv, %	selectivity (gluconic acid), %
1000	1 h	79.6	91.2
1000	2 h	92.4	87.5
500	1 h	99.0	88.1
100	15 min	>99.9	91.9

[a]Reaction conditions: H_2O = 20 mL, catalyst = 0.0396 g, T = 383 K, $P(O_2)$ = 0.3 MPa.

In addition, we have also tried hydrogen peroxide as oxidant in this pressure bottle system, and the results are as expected. When the reaction temperature was set as 333 K and equimolecular hydrogen peroxide was given, the conversion was ~29.0%, with almost full selectivity. As was mentioned previously, when the temperature was lower than 333 K, no byproduct was produced, and high selectivity toward gluconic acid could be achieved. However, when the temperature was increased to 383 K, with an increasing conversion of 85.4%, the selectivity toward gluconic acid decreased to 84.7%. This change was in accordance with the situation when oxygen was used as oxidant, indicating that isomerization happened as well on this occasion. We also conducted an experiment at 333 K with bubbling oxygen. No fructose was generated when no NaOH was added. However, if equimolecular NaOH was added before the reaction, fructose could be observed in the reaction liquid, despite the low temperature and atmospheric pressure, because there was a large amount of hydroxyl ions existing in the solution.

It is speculated that the generation of fructose is controlled by both temperature and hydrogen peroxide. Only in the case when both the temperature and concentration of hydrogen peroxide are high enough could the produced hydroxyl ions reach the amount to make isomerization happen. In addition, because of the acidic condition of the reaction system, the produced hydroxyl ions may not exist for a long time. Therefore, hydroxyl ions may disappear before isomerization happens when its concentration is not high enough.

Back to the above experiment carried out at 383 K with hydrogen peroxide as oxidant, although the conversion was lower compared with the situation using oxygen as oxidant, the selectivity was also lower. This might be ascribed to the higher concentration of hydrogen peroxide existing in the reaction system, which would produce more hydroxyl ions. Previously, some authors have tested gold catalysts in glucose oxidation using hydrogen peroxide as oxidant and achieved high selectivity toward gluconic acid. However, the experiments were all conducted at very low temperatures and well-controlled pH values. For example, the reactions were carried out at 313 K with the pH fixed at 9 in Prüße's works[42,43] and at 303 K with a pH of 9.5 in Haruta's work.[44] Under these circumstances, according to our speculation, high selectivities toward gluconic acid could naturally be achieved. Nevertheless, even if various experiments have been conducted to support this mechanism, we are not quite certain about its correctness. Because the key factor that is the hydroxyl ion can hardly be detected as a result of its instability, this mechanism may be only a hypothesis at present.

DOI: 10.1021/cs502093b
ACS Catal. 2015, 5, 2659−2670

4. CONCLUSIONS

This study showed that the Au/CMK-3 catalyst had an advantage in the aerobic oxidation of glucose under base-free conditions. Increasing the temperature and oxygen pressure could promote the reaction rate and conversion, and the improving effect was more obvious when the oxygen pressure was increased at a relatively high temperature. At 383 K and 0.3 MPa, the conversion could exceed 92% in 2 h. Furthermore, the amount of the byproduct fructose was affected by the generation of hydrogen peroxide, which was produced simultaneously in the main reaction. Thus, for a catalyst under a fixed reaction condition, the selectivity reduced gradually along with time, but for the different catalysts that reached the same conversion, the one that cost less time would have a better selectivity toward gluconic acid.

The stability of the Au/CMK-3 catalyst was studied. The conversion dropped gradually from 92% to ~70% through the four subsequent runs. Two different kinds of regeneration method, including NaOH treatment and calcination, were compared and discussed. On the basis of the results, the used catalyst treated with 50 mL of 0.1 mol/L NaOH for 30 min at 363 K showed the best performance with 87% conversion. The characterizations indicated that after the recycling experiments, abundant carboxylic acids were adsorbed on the surface of the catalyst, which was the predominant factor that caused deactivation. Both NaOH treatment and calcination could effectively remove the adsorbates, and atmospheric calcination was more useful in this aspect. However, given the appearance of large particles during the calcination procedure, the consequence was no match for the NaOH treatment method. Therefore, one can conclude that the NaOH treatment is a very simple but useful way to regenerate used catalysts that suffered from adsorbate deactivation in glucose oxidation.

■ ASSOCIATED CONTENT

Supporting Information

The following file is available free of charge on the ACS Publications website at DOI: 10.1021/cs502093b.

N_2 adsorption−desorption isotherms, XRD patterns, TEM images and CO_2-TPD profiles of some catalysts as well as the recycling experiment data (PDF)

■ AUTHOR INFORMATION

Corresponding Author

*Phone: +86-592-2181659. Fax: +86 592 2183047. E-mail: yzyuan@xmu.edu.cn.

Notes

The authors declare no competing financial interest.

■ ACKNOWLEDGMENTS

We acknowledge the financial supports from the MOST of China (2011CBA00508), the NSFC (21403178 and 21473145), the Research Fund for the Doctoral Program of Higher Education (20110121130002), and the Program for Changjiang Scholars and Innovative Research Team in University (IRT_14R31).

■ REFERENCES

(1) Gallezot, P. *Catal. Today* **2007**, *121*, 76−91.
(2) Ma, C. Y.; Xue, W. J.; Li, J. J.; Xing, W.; Hao, Z. P. *Green Chem.* **2013**, *15*, 1035−1041.
(3) Hustede, H.; Haberstroh, H.-J.; Schinzig, E. In *Ullmann's Encyclopedia of Industrial Chemistry*, 6th ed.; Wiley-VCH: Weinheim, 2000; Vol. *A 12*, pp 449−456.
(4) Thielecke, N.; Aytemir, M.; Prüsse, U. *Catal. Today* **2007**, *121*, 115−120.
(5) Baatz, C.; Prüße, U. *J. Catal.* **2007**, *249*, 34−40.
(6) Lichtenthaler, F. W. In *Biorefineries — Industrial Processes and Products*, 1st ed.; Kamm, B.; Gruber, P. R.; Kamm, M., Eds.; Wiley-VCH: Weinheim, 2008; Vol. 2, pp 2−5.
(7) Kobayashi, H.; Fukuoka, A. *Green Chem.* **2013**, *15*, 1740−1763.
(8) Dirkx, J. M. H.; van der Baan, H. S. *J. Catal.* **1981**, *67*, 1−13.
(9) Besson, M.; Lahmer, F.; Gallezot, P.; Fuertes, P.; Fleche, G. *J. Catal.* **1995**, *152*, 116−121.
(10) Wenkin, M.; Ruiz, P.; Delmon, B.; Devillers, M. *J. Mol. Catal. A, Chem.* **2002**, *180*, 141−159.
(11) Gallezot, P. *Catal. Today* **1997**, *37*, 405−418.
(12) Pina, C. D.; Falletta, E.; Rossi, M. *Chem. Soc. Rev.* **2012**, *41*, 350−369.
(13) Kusema, B. T.; Murzin, D. Y. *Catal. Sci. Technol.* **2013**, *3*, 297−307.
(14) Biella, S.; Prati, L.; Rossi, M. *J. Catal.* **2002**, *206*, 242−247.
(15) Hermans, S.; Devillers, M. *Appl. Catal., A* **2002**, *235*, 253−264.
(16) Comotti, M.; Pina, C. D.; Falletta, E.; Rossi, M. *Adv. Synth. Catal.* **2006**, *348*, 313−316.
(17) Zhang, H. J.; Okuni, J.; Toshima, N. *J. Colloid Interface Sci.* **2011**, *354*, 131−138.
(18) Mirescu, A.; Berndt, H.; Martin, A.; Prüße, U. *Appl. Catal., A* **2007**, *317*, 204−209.
(19) Thielecke, N.; Vorlop, K.-D.; Prüße, U. *Catal. Today* **2007**, *122*, 266−269.
(20) Wang, Y. R.; Van de Vyver, S.; Sharma, K. K.; Román-Leshkov, Y. *Green Chem.* **2014**, *16*, 719−726.
(21) Miedziak, P. J.; Alshammari, H.; Kondrat, S. A.; Clarke, T. J.; Davies, T. E.; Morad, M.; Morgan, D. J.; Willock, D. J.; Knight, D. W.; Taylor, S. H.; Hutchings, G. J. *Green Chem.* **2014**, *16*, 3132−3141.
(22) Dimitratos, N.; Villa, A.; Wang, D.; Porta, F.; Su, D.; Prati, D. *J. Catal.* **2006**, *244*, 113−121.
(23) Skupien, E.; Berger, R. J.; Santos, V. P.; Gascon, J.; Makke, M.; Kreutzer, M. T.; Kooyman, P. J.; Moulijn, J. A.; Kapteijn, F. *Catalysts.* **2014**, *4*, 89−115.
(24) Wang, T.; Shou, H.; Kou, Y.; Liu, H. *Green Chem.* **2009**, *11*, 562−568.
(25) Ding, Y.; Li, X. H.; Pan, H. Y.; Wu, P. *Catal. Lett.* **2014**, *144*, 268−277.
(26) Sun, F.; Liu, J.; Chen, H. C.; Zhang, Z. X.; Qiao, W. M.; Long, D. H.; Ling, L. C. *ACS Catal.* **2013**, *3*, 862−870.
(27) Saha, D.; Deng, S. G. *Langmuir* **2009**, *25*, 12550−12560.
(28) Zhao, D. Y.; Feng, J. L.; Huo, Q. S.; Melosh, N.; Fredrickson, G. H.; Chmelka, B. F.; Stucky, G. D. *Science* **1998**, *279*, 548−552.
(29) Jun, S.; Joo, S. H.; Ryoo, R.; Kruk, M.; Jaroniec, M.; Liu, Z.; Ohsuna, T.; Terasaki, O. *J. Am. Chem. Soc.* **2000**, *122*, 10712−10712.
(30) Bi, Q.-Y.; Du, X.-L.; Liu, Y.-M.; Cao, Y.; He, H.-Y.; Fan, K.-N. *J. Am. Chem. Soc.* **2012**, *134*, 8926−8933.
(31) Cui, H.-F.; Ye, J.-S.; Liu, X.; Zhang, W.-D.; Sheu, F.-S. *Nanotechnology* **2006**, *17*, 2334−2339.
(32) Zhe, Y. Q.; Ma, C. A.; Zhu, Y. H. *Acta Phys. Chim. Sin.* **2004**, *20*, 331−335.
(33) Zhang, X.; Cui, Y.; Lv, Z.; Li, M.; Ma, S.; Cui, Z.; Kong, Q. *Int. J. Electrochem. Sci.* **2011**, *6*, 6063−6073.
(34) Önal, Y.; Schimpf, S.; Claus, P. *J. Catal.* **2004**, *223*, 122−133.
(35) Datsyuk, V.; Kalyva, M.; Papagelis, K.; Parthenios, J.; Tasis, D.; Siokou, A.; Kallitsis, I.; Galiotis, C. *Carbon* **2008**, *46*, 833−840.
(36) Avilés, F.; Cauich-Rodríguez, J. V.; Moo-Tah, L.; May-Pat, A.; Vargas-Coronado, R. *Carbon* **2009**, *47*, 2970−2975.
(37) Zhang, J.; Jin, Y.; Li, C. Y.; Shen, Y. N.; Han, L.; Hu, Z. X.; Di, X. W.; Liu, Z. L. *Appl. Catal., B* **2009**, *91*, 11−20.
(38) Kvande, I.; Zhu, J.; Zhao, T.-J.; Hammer, N.; Rønning, M.; Raaen, S.; Walmsley, J. C.; Chen, D. *J. Phys. Chem. C* **2010**, *114*, 1752−1762.

DOI: 10.1021/cs502093b
ACS Catal. 2015, 5, 2659−2670

(39) Wan, X. Y.; Zhou, C. M.; Chen, J. S.; Deng, W. P.; Zhang, Q. H.; Yang, Y. H.; Wang, Y. *ACS Catal.* **2014**, *4*, 2175−2185.
(40) Kundu, S.; Wang, Y. M.; Xia, W.; Muhler, M. *J. Phys. Chem. C* **2008**, *112*, 16869−16878.
(41) Weiss, J. *Trans. Faraday Soc.* **1935**, *31*, 1547−1557.
(42) Saliger, R.; Decker, N.; Prüße, U. *Appl. Catal., B* **2011**, *102*, 584−589.
(43) Prüße, U.; Jarzombek, P.; Vorlop, K.-D. *Top Catal.* **2012**, *55*, 453−459.
(44) Ishida, T.; Kuroda, K.; Kinoshita, N.; Minagawa, W.; Haruta, M. *J. Colloid Interface Sci.* **2008**, *323*, 105−111.

DOI: 10.1021/cs502093b
ACS Catal. 2015, 5, 2659−2670